Thermal and electrical conductivity of melt mixed polycarbonate hybrid composites co-filled with multi-walled carbon nanotubes and graphene nanoplatelets.

SCHOLARONE™
Manuscripts

Graphical abstract
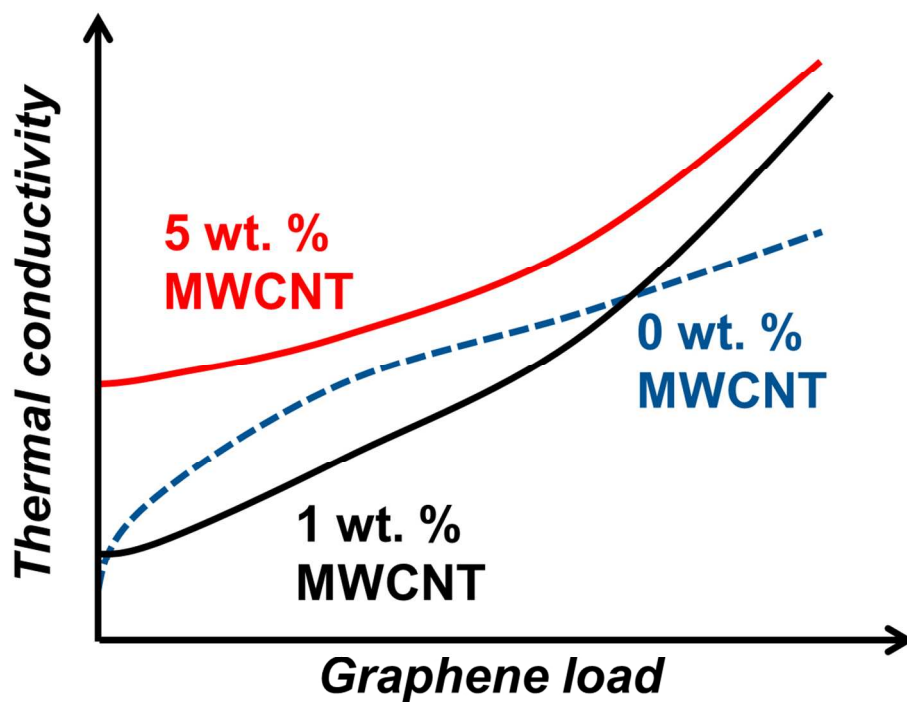228x178mm (150 x 150 DPI)

Thermal and electrical conductivity of melt mixed polycarbonate hybrid composites co-filled with multi-walled carbon nanotubes and graphene nanoplatelets.

Marcin Wegrzyn [a]*, Amaya Ortega [a], Adolfo Benedito [a], Enrique Gimenez [b]

[a] Instituto Tecnológico del Plástico (AIMPLAS), Calle Gustave Eiffel 4, 46980 Paterna, Spain

[b] Instituto de Tecnología de Materiales. Universidad Politécnica de Valencia, Camino de Vera, 46022 Valencia, Spain

Correspondence: e-mail: *marcinwegrzyn@hotmail.com*

ABSTRACT

In this work, we present thermoplastic nanocomposites of polycarbonate (PC) matrix with hybrid nanofillers system formed by a melt-mixing approach. Various concentrations of multi-wall carbon nanotubes (MWCNT) and graphene nanoplatelets (GnP) were mixed in to polycarbonate and the melt was homogenized. The nanocomposites were compression molded and characterized by different techniques. Torque dependence on the nanofiller composition increased with the presence of carbon nanotubes. The synergy of carbon nanotubes and graphene nanoplatelets showed exponential increase of thermal conductivity, which was compared to logarithmic increase for nanocomposite with no MWCNT. Decrease of Shore A hardness at elevated loads present for all investigated nanocomposites was correlated with the expected low homogeneity caused by a low shear during melt-mixing. Mathematical model was used to calculate elastic modulus from Shore A tests results. Vicat softening temperature showed opposite pattern for hybrid nanocomposites and for PC-MWCNT increasing in the latter case. Electrical conductivity boost was explained by the collective effect of high nanofiller loads and synergy of MWCNT and GnP.

INTRODUCTION

Thermoplastic polymer composites filled with carbon-based nanomaterials offer many solutions for material science. [1] Significant improvement of electrical and thermal properties of insulating polymers in these nanocomposites is attributed to the carbon nanotubes or graphene nanoplatelets used as filler. [2,3] A unique structure of these nanofillers provides also good mechanical performance of nanocomposites. [4,5] These two aforementioned

nanomaterials, often used separately as fillers, [6,7] recently gained more attention as components of a hybrid systems-based nanocomposites. [8,9] Complex engineering materials formed by co-filling thermoplastics with one- and two-dimensional fillers provide a broad range of opportunities for science and technology. However, a good quality interconnected network of nanofillers is necessary to reach the desired improvement of properties. The main problem distracting the performance of MWCNT and GnP is inefficient energy applied during processing disabling the breakage of nanofiller macrostructures causing inhomogeneous morphology of the final nanocomposite. [10] This is related to the breakage of primary carbon nanotube agglomerates in the process of macrostructure penetration by polymer melt [11] or graphite exfoliation in order to obtain monolayer sheets of graphene nanoplatelets. [12] In a common nanocomposite formation by melt-mixing the energy input is usually controlled by the parameter: specific mechanical energy (SME). [13] Nevertheless, SME is convenient mainly for a continuous process and can be replaced in parameters influence analysis by torque. This is a desired solution when an internal mixer is used instead of a twin-screw extruder or when high nanofiller loads are used disabling microscopic methods of morphology determination. [14]

Intrinsic thermal conductivity of polymer-based materials is a key feature for processing and for application. [15] Exfoliated or expanded graphene is reported to give good results improving the thermal conductivity of thermoplastic materials. The performance depends on the aspect ratio of the individual particles [16] and the dispersion quality in the matrix. [17] However, often high volume fractions of nanofillers are necessary for the desired increase of thermal conductivity which restricts some of the commonly used processing methods such as extrusion or injection molding. [18] Therefore, hybrid nanocomposites are the optimal solution to decrease filling load with maintaining comparable thermal properties. [19] Hybrid

fillers additionally induce morphological changes in the matrix (*e.g.* chains alignment) which has a positive effect on the thermal conductivity. [20] A reported synergistic effect of carbon nanotubes and graphene in epoxy matrix show greater increase of thermal conductivity and mechanical properties for co-filled nanocomposites than for nanocomposites individually filled with each of these nanofillers. [21] Besides, Vicat hardness as a parameter defining polymer softening point is improved with carbon nanotubes content which is reported for commodity polymers like PP obtained by a twin-screw extrusion. [22] However, the balance of properties occurs at low loads (1-3 wt. %) which suggests the occurrence of percolation threshold. Opposite observations reported for non-carbonous fillers show a decreasing Vicat softening point with an increase of volume fraction. [23] Shore A hardness showing the values measured at room temperature increases with carbon nanotubes [24] and with two-dimensional silicate [25] concentration increase. Nevertheless, the change observed was clearly higher for the hybrid system combining these nanofillers. A correlation between the elastic modulus in compression and Shore A hardness was reported with a mathematical simulation of experimental data giving an acceptable agreement with *ca.* 5% error. [26] Thus, the theory of Boussinesq for comparison of both data sets is adequate. Furthermore, no modification of Shore A method in order to correlate the data with elastic modulus [27] was necessary. The aforementioned reports confirm that the dependence of mechanical performance on the various one- and two-dimensional fillers in a hybrid system exists. This is reported especially for the low-to-moderate filler concentrations.

In this work, we present PC-MWCNT/GnP nanocomposites prepared by melt-mixing in an internal mixer. Various nanofiller content and mutual nanofillers ratio allow studying the influence of synergistic effect on thermal and electrical conductivity. The study of torque during the nanocomposites formation shows the influence of nanofillers composition.

Thermal conductivity and thermal effusivity were determined on a compression molded

specimens with a Modified Transient Plane Source (MTPS) approach. Hardness measured at

room temperature (Shore A) and Vicat hardness were determined in order to observe the

influence of carbon nanotubes and graphene nanoplatelets in hybrid system. A simple

mathematical model was used in order to calculate the elastic modulus in compression from

Shore A test data. Electrical conductivity measured with a two-point contact method is given

in order to correlate electrical and thermal performance of the nanocomposites.

EXPERIMENTAL

- *Materials*

Commercial polycarbonate (PC) Lexan ELX 6013 (MVR 5 g/10min) was supplied by SABIC

Innovative Plastics. Multi-walled carbon nanotubes (MWCNT) NC7000 with average

diameter 9.5 nm and average length 1.5 μm were supplied by Nanocyl. Graphene

nanoplatelets (GnP) xGnP-M5 with thickness 6-8 nm and average particle diameter 5 μm

were supplied by XG Sciences.

- *Preparation of nanocomposites*

Nanocomposites with various nanofillers concentrations shown in Table 1 were prepared on

a Brabender Plasti-Corder PL-2000 internal mixer at screw speed 120 rpm and barrel

temperature 280 °C. Polycarbonate (PC) was introduced to the mixing chamber and blended

for 1 min until the torque was constant. Carbon nanotubes (MWCNT) and graphene

nanoplatelets (GnP) were added to melted polycarbonate (PC) after this time and such

formed nanocomposite was mixed for 9 minutes. PC-MWCNT/GnP nanocomposites

subtracted from the mixing cavity were compression molded at 280 $^\circ$C on a Collin 6300

hydraulic press into the rectangular specimens with dimensions 25x25x5 mm^3. A 25 min

compression process was composed of five-steps with applied pressures varied between 5

bar and 140 bar.

- *Characterization*

The tests were carried out on the compression molded specimens. Thermal conductivity of

the nanocomposites was measured on a TCi TH89 Modified Transient Plane Source (MTPS)

thermal conductivity analyzer (C-Therm Technologies). A one-sided heat reflectance sensor

shown in Figure 1a provides a controlled amount of heat changing the temperature of a

sample surface inducing the voltage drop. Two measurements (Figure 1b) were carried out

for each of the five rectangular specimens at ambient temperature (26.1 ± 0.5°C) with

deionized water used as a contact medium. Individual test included data collection step of

0.8 s and sensor cooling step between the data acquisition of 60 s.

Hardness of the nanocomposites was measured on an A-type Shore durometer. In this

method a standardized intender was pressed by 8.064 N force into the specimen for 15 s at

ambient temperature. After this time the hardness was determined based on the depth of

indentation. Mathematical model was introduced in order to calculate the Elastic modulus

from the hardness data.

Vicat softening point was determined with B50 method following the EN ISO 306 standard.

In this method a flat-ended needle was constantly pressed by 50 N force into the specimen.

Temperature of silicon oil used as a medium was raised from ambient with a rate 50 $^{\circ}$C h^{-1}.

Electrical resistivity was measured by a two-point contact configuration on a Keithley 2000

Multimeter source/meter. Silver electrodes were painted on the samples in order to

improve contact between the specimen and the measuring electrodes.

RESULTS AND DISCUSSION

Each of the hybrid nanocomposites filled with carbon nanotubes (MWCNT) and graphene

nanoplatelets (GnP) prepared with a single, ten minutes-long processing step shows a

decrease of torque with the homogenization of the melt (Figure 2 and Table 2). The curves in

Figure 2 represent torque during the formation of selected PC-GnP nanocomposites with no

carbon nanotubes. A clear increase of torque representing the melt resistance to

deformation during mixing increases with the nanofiller load until 10.0 wt. % GnP. A change

of nanocomposite behavior for material 0T/15G is explained by the lubricating properties of

graphite, stronger at elevated loads. A 10.0 wt. % GnP seems to be the limit above which the

agglomerates are large enough to disable strong nano-scale interactions between graphene

and polymer chains. Besides, intensification of the lubricating properties of graphene [28] at

elevated loads facilitates the laminar flow of polymer melt in discrete layers. [29] Furthermore,

the torque seems to be more constant above the 8th minute of processing (7th minute of the

nanocomposite mixing) for each investigated GnP concentration present in Figure 2. This

reduction of the curve slope indicates the point of the formation of a relatively

homogeneous nanocomposite. No significant improvement is expected with the increase of

mixing time at the applied conditions, as from this moment the degradation of polymer matrix causing polymer chains shortening competes with the improvement of the nanofiller dispersion. On the contrary, the torque observed for polycarbonate decreases consecutively with the processing time and no plateau occurs, suggesting the influence of a slight polymer degradation caused by the temperature and the shear.

Further increase of torque is observed when carbon nanotubes are introduced to the system together with graphene (Table 2). During each individual process the torque behaves similarly to PC-GnP and an increase with nanofillers load is observed. Besides, the plateau observed for PC-GnP started at the 8th minute of processing does not occur when carbon nanotubes are introduced. Such an effect is most probably related to inhomogeneous nanofillers dispersion after this processing time. Therefore, the processing time for hybrid nanocomposites formation in internal mixer should be balanced providing good dispersion of nanofillers and the lowest possible matrix degradation. Data present in Table 2 shows much stronger increase of torque between 1T/1G and 1T/0G than for the further increase of GnP content. A *ca.* 13 % torque increase is observed when 1.0 wt. % GnP is introduced to the PC-GnP (creating 1T/1G) and 8 % increase for the 5.0 wt. % GnP (1T/5G) and 10.0 wt. % GnP (1T/10G). This observation is confirmed also for the nanocomposites with 5.0 wt. % MWCNT but the increase of torque is minor. Such an effect is related mainly to the type of nanofiller. Addition of graphene nanoplatelets causes the formation of interconnected hybrid network increasing the viscosity of the nanocomposite. Besides, nanocomposites with the total nanofiller loads between 1.0 wt. % and 2.0 wt. % are most likely in the range of mechanical percolation, which should show the observed effect on torque. Similarly to the materials with no carbon nanotubes shown in Figure 2, the lower values of torque were observed for

nanocomposites 1T/15G than for 1T/10G. This is understood as a strong impact of the high load of graphene nanoplatelets.

Besides, the nanocomposite 0T/1G (Figure 2) shows higher torque value than 1T/0G (Table 2). The difference of *ca.* 6 % observed above the 6th minute of processing indicates that at the low nanofiller loads the nanocomposite filled with graphene causes more obstacles for the mixer. This may be caused by the better dispersion and thus stronger interactions between the nanomaterial and polymer chains. Nevertheless, at low loads the penetration of carbon nanotube agglomerates by polymer melt leading to the individually-dispersed nanoparticles seems to be easier than a good dispersion of graphene nanoplatelets including the previous exfoliation. Reports show improved dispersion ability of nanomaterials in some hybrid systems. [30,31] A relatively low shear rate during the nanocomposites preparation suggests a non-efficient MWCNT agglomerates breakage and the formation of incomplete network in polymer matrix. Opposite effect with the synergy between carbon nanotubes and graphene nanoplatelets is observed in nanocomposites with the high total nanofiller load (6.0 wt. %): 1T/5G and 5G/1T. Summarizing, the torque increases with an increase of MWCNT load and a decrease of GnP load. Material behavior changes at high nanofiller concentration so the efficiency of graphene nanoplatelets dispersion in polymer matrix is reduced. [32]

Thermal conductivity measured by the Modified Transient Plane Source (MTPS) approach (Figure 1) increases with the total nanofiller load for all investigated nanocomposites (Figure 3). The expected higher values for the hybrid compositions containing 5.0 wt. % MWCNT were observed along the whole series. The curves recorded for the hybrid nanocomposites follow an exponential function while the curve obtained for the PC-GnP is logarithmic. For

the hybrid nanocomposites with 1.0 wt. % MWCNT thermal conductivity is generally lower

than for the PC filled only with graphene nanoplatelets. This is attributed to the

aforementioned synergy causing the decrease of torque for 1T/5G comparing to 5T/1G

(Table 2), having origins in the dispersion ability of one nanomaterial with the presence of

another. Besides, the alignment of nanofiller is reported to play a key role in thermal

conductivity performance of nanocomposites. [33] Such behavior is expected to change at high

loads and for the material 1T/15G thermal conductivity is higher than for the 0T/15G. The

effect of the increase of thermal conductivity at such high NgP load with the presence of 1.0

wt. % MWCNT is probably related to the amount rather than the type of nanofiller.

A parameter K_{nc}/K_{mx} often used to represent the efficiency of material treatment on thermal

properties is a ratio between the obtained thermal conductivity (K_{nc}) and thermal

conductivity of a neat matrix (K_{mx}), a 0.261 WmK^{-1} for polycarbonate. Value generally

increases with the increase of MWCNT and GnP load. Thus, regarding the highest studied

graphene nanoplatelets load of 15.0 wt. %, the K_{nc}/K_{mx} gives values between 2.79 (0T/15G)

and 3.33 (5T/15G). For significantly lower GnP concentration 1.0 wt. %, K_{nc}/K_{mx} is between

1.23 (0T/1G) and 1.83 (5T/1G). This behavior is confronted with the PC-MWCNT

nanocomposite without graphene nanoplatelets and no significant change is observed for

1.0 wt. % MWCNT before and after the addition of GnP (1T/0G and 1T/1G, respectively). This

confirms the importance of the hybrid nanofiller system at high concentrations in order to

boost the thermal conductivity of insulating polymer matrix.

Thermal effusivity of nanocomposites e_{nc} defined by Equation 1 is present in Table 3. The

values agree with the previous observations of thermal conductivity performance. The ability

of the nanocomposite to absorb/exchange heat depends on the thermal conductivity of this

nanocomposite K_{nc}, its density ρ_{nc} and the specific heat capacity c_p. A nearly linear increase

of the thermal effusivity with an increase of graphene nanoplatelets content is observed for

the nanocomposites with no carbon nanotubes. Introduction of MWCNT and the formation

of hybrid nanocomposites results with the exponential increase of effusivity with the

increase of GnP load. Such a non-linear dependence is related to the presence of MWCNT-

GnP interconnected network where a synergy of the hybrid nanofiller system increases the

possible number of contacts between the particles. From a defined concentration the

thermal performance changes significantly with a slight increase of the load. At 15.0 wt. %

GnP (1T/15G and 5T/15G) the thermal effusivity is almost equal for both nanocomposites,

showing only 16.3 % difference. This agrees with the aforementioned statement regarding

upper level of the efficient nanofiller load.

$$e_{nc} = \left(K\rho_{nc}c_p\right)^{1/2} \qquad\qquad\qquad (1)$$

Hardness of the nanocomposites measured by a Shore type A method is shown in Figure 4.

An initial improvement of hardness is observed with the introduction of 1.0 wt. % GnP, for

materials 0T/1G and 1T/1G. The value between these nanocomposites does not differ

significantly due to the effect of low nanofiller load. [34] Further development of the

nanocomposites show that hardness decreases significantly, below the value recorded for

the neat polycarbonate. Further increase of the total nanofiller load for both series shown in

Figure 4 indicated the relative similarity between the material with 0.0 wt. % MWCNT and

the material with 5.0 wt. % MWCNT occurs at low (1.0 wt. %) and high (15.0 wt. %) GnP

concentrations. Nevertheless, the values are clearly lower for PC-GnP than for the hybrid

nanocomposite with 1.0 wt. % MWCNT which confirms the aforementioned synergy. Besides,

literature reports show the optimal size of grains in polymer matrix d_c=10 nm providing the

highest hardness. [35] The decrease of hardness below and above that defined grain size is

correlated with the inter-granular processes. This theory can be adapted to the

nanocomposites where a well-dispersed nanofiller phase meets the d_c requirement. [36] Thus,

it seems that the concentration of macrostructures (micro-scale agglomerates) in the

studied polycarbonate nanocomposites at GnP loads above 5.0 wt. % is relatively high.

Therefore, the explanation of the decrease of Shore A hardness can be related to the

inhomogeneity of the material at elevated nanofiller loads. [37] However, at such high

concentrations of carbon nanomaterials the transparency of the nanocomposite disables any

statistically-supported analyses of micrographs revealing the quality of the morphology.

Modulus of elasticity in compression present in Table 4 is determined basing on a Shore A

hardness results. [26] Equation 2 defining the relationship between these parameters (E and

Sh_A, respectively) includes the normalized radius of the indenter R=0.395 mm, Poisson's ratio

μ=0.5 and constants related to the relation between the depth of penetration and the Shore

A hardness: C_1=0.549 N, C_2=0.07516 N and C_3=0.025 mm. A standard deviation between the

mathematical model and the experimental data is 5.4%. [26] Results of calculation show an

increase (*ca.* 2.5 %) of polycarbonate elastic modulus in compression after the formation of

0T/1G and 1T/1G. This initial increase of elastic modulus, analogous to the Shore A hardness,

is followed by a significant decrease at elevated total nanofiller loads. A clear reduction of E

is calculated with relatively high accuracy and can be related to the size of filler

agglomerates. At elevated loads both nanofillers tend to exist in nanocomposites in the form

of macrostructures, which causes a decrease of mechanical properties of the final material.

$$E = \frac{1-\mu^2}{2 \cdot R \cdot C_3} \cdot \frac{C_1 + C_2 \cdot Sh_A}{100 - Sh_A} \cdot (2.6 - 0.02 \cdot Sh_A) \qquad (2)$$

Figure 5 with the Vicat softening temperature (VST) of the selected nanocomposites shows a behavior strongly dependent on the presence of carbon nanotubes. Literature reports confirm an increase of the softening temperature with the increase of carbon nanotube or the other co-filler content. [22,38] This behavior is also observed for the hybrid PC-MWCNT/GnP nanocomposites at 1.0 wt. % MWCNT and 1.0 wt. % GnP (1T/1G). An optimal load below 3.0 wt. % nanofiller is reported to show the best Vicat temperature improvement for various nanofillers, which is in agreement with the findings present here. [22,38] Further increase of graphene nanoplatelets concentration with the presence of 1.0 wt. % carbon nanotubes causes the decrease of softening temperature. This behavior is opposite when no MWCNT is present in the matrix, which confirms stronger impact of graphene on VST due to a plate-like structure. Besides, the low value of VST is observed for 1T/10G and 1T/15G is similar and higher than a VST for 1T/0G. It seems that the aforementioned optimal load should be also selected for hybrid nanocomposites and a synergistic effect needs to be considered.

Electrical conductivity values of the hybrid PC-based nanocomposites measured by a two-point method described elsewhere [39] are shown in in Figure 6 and in Table 5. The improvement of electrical properties of PC/GnP in Table 5 shows the performance of a 4 orders of magnitude increase of the virgin polycarbonate value for 1.0 wt. % GnP (0T/1G). Besides, a significant improvement of electrical conductivity with graphene nanoplatelets concentration occurs for both studied carbon nanotube loads (Figure 6). A 33.2 % increase

between 1T/0G and 1T/15G or a 167.0 % increase between 5T/0G and 5T/15G shows the

possible performance of the studied hybrid nanofiller system. Furthermore, a difference

between the nanofillers is clear when the electrical conductivity performance for the same

concentration is compared. The 0T/1G shows an increase of a *ca.* 10^4 Scm^{-1} of the PC value,

while the 1T/0G gives 10^{13} Scm^{-1}. Nevertheless, the effect of a hybrid system does not show

significant difference favoring one nanofiller or another. Nanocomposite 1T/5G shows 1.0E-

01 Scm^{-1} while 5T/1G: 4.1E-01 Scm^{-1}. Such a boost observed for PC-MWCNT/GnP is

attributed to a collective effect of high total nanofillers load and to the formation of

interconnected hybrid network including two different types of nanofiller: one-dimensional

nanotubes and two-dimensional flakes. Furthermore, a rather low shear during the whole

processing does not affects the length of carbon nanotubes which is beneficial for the

formation of the interconnected nanofillers network. Shortening of carbon nanotubes is

reported to distract significant improvement of carbon nanotubes-based nanocomposites. [37]

CONCLUSIONS

Polycarbonate-based nanocomposites with a hybrid nanofillers system including multi-wall

carbon nanotubes (MWCNT) and graphene nanoplatelets (GnP) show improvement of

thermal and electrical conductivity of the virgin matrix. The nanocomposites with moderate-

to-high loads of GnP provide significantly lower torque during melt mixing than the

nanocomposites containing also MWCNT. Such effect was attributed to the synergy between

nanoparticles resulting in the formation of interconnected hybrid network that increases

viscosity and hampers screws rotation. Exponential boost of the thermal conductivity was

explained with similar effect giving a 0.869 WmK^{-1} for hybrid PC nanocomposite with 15.0 wt.

% GnP and 5.0 wt. % MWCNT and 0.728 WmK^{-1} with the absence of carbon nanotubes. This

is an increase of polycarbonate value on the level of 233% and 180%, respectively. Hardness

obtained in a Shore A test, used also to determine elastic modulus in compression,

decreased at elevated nanofiller concentrations even though an increase of the matrix value

was recorded below the total nanofiller load of 5.0 wt. %. Observation of the reduction of

Vicat softening temperature for hybrid nanocomposites and the increase for PC-MWCNT is

related with the insufficient shear provided during the formation of nanocomposite causing

limited ability of agglomerates breakage and graphene exfoliation. A correct mutual

concentration of nanofillers should be selected in order to achieve highest values of the

studied parameters. Electrical conductivity boost was observed to be dependent on the

presence of carbon nanotubes and showed the collective effect of high nanofiller loads and

synergy between carbon nanotubes and graphene nanoplatelets.

REFERENCES

[1] Su, I.; Schlögl, R. *Chem. Sus. Chem.* **2010**, 3, 136-168.

[2] Yang, L.; Liu, F.; Xia, H.; Qian, X.; Shen, K.; Zhang, J. *Carbon* **2011**, 49, 3274-3283.

[3] Singh, I.V.; Tanaka, M.; Endo M. *Int. J. Therm. Sci.* **2007**, 46, 842-847.

[4] Kuan, H.C.; Ma, C.C.M.; Chang, W.P.; Yuen, S.M.; Wu, H.H.; Lee, T.M. *Comp. Sci. Tech.* **2005**, 65, 1703-1710.

[5] Arasteh, R.; Omidi, M.; Rousta, A.H.A.; Kazerooni, H. *J. Macromol. Sci. B* **2011**, 50, 2464-2480.

[6] Wegrzyn, M.; Benedito, A.; Gimenez, E. *J. Appl. Polym. Sci.* **2014**, 131, 40271-40279.

[7] Cai, D.; Jin, J.; Yusoh, K.; Rafiq, R.; Song, M. *Compos. Sci. Technol.* **2012**, 72, 702-707.

[8] Martin-Gallego, M.; Verdejo, R.; Khayet, M.; Ortiz de Zarate, J.M.; Essalhi, M.; Lopez-Manchado, M.A. *Nanoscale Res. Lett.* **2011**, 610, 1-7.

[9] Yu, D.; Dai, L. *J. Phys. Chem. Lett.* **2010**, 1, 467-470.

[10] Haslam, M.D.; Raeymaekers, B. *Comp. B* **2013**, 55, 16-21.

[11] Pötschke, P.; Dudkin, S.M.; Alig, I. Polymer **2003**, 44, 5023-5030.

[12] Stankovich, S.; Dikin, D.A.; Dommett, G.H.; Kohlhaas, K.M.; Zimney, E.J.; Stach, E.A.; Piner, R.D.; Nguyen, S.T.; Ruoff, R.S. *Nature* **2006**, 442, 282-286.

[13] Sathyanarayana, S.; Olowojoba, G.; Weiss, P.; Calgar, B.; Pataki, B.; Mikonsaari, I.; Huebner, C.; Hening, F. *Macromol. Mater. Eng.* **2013**, 298, 89-105.

[14] Ye, L.; Wu, Q.; Qu, B. *Polym. Degrad. Stabil.* **2009**, 94, 751-756.

[15] Ebadi-Dehaghani, H.; Nazempour, M. In Smart Nanoparticles Technology - Thermal Conductivity of Nanoparticles Filled Polymers; Hashim, A., Eds.; InTech, **2012**, pp. 519-540.

[16] Kalaitzidou, K.; Fukushima, H.; Drzal, L. *Carbon* **2007**, 45, 1446-1452.

[17] Mu, Q.; Feng, S.; Diao, G. *Polym. Compos.* **2007**, 28, 125-130.

[18] King, J.A.; Barton, R.L.; Hauser, R.A.; Keith, J.M. *Polym. Compos.* **2008**, 29, 421-428.

[19] Hwang, Y.; Kim, M.; Kim, J. *Compos Part. A – Appl. S.* **2013**, 55, 195-202.

[20] Babaei, H.; Keblinski, P.; Khodadadi, J.M. *Inter. J. Heat Mass Tran.* **2013**, 58, 209-216.

[21] Yang, S.Y.; Lin, W.N.; Huang, Y.L.; Tien, H.W.; Wang, J.Y.; Ma, C.C.M.; Li, S.M.; Wang, Y.S. *Carbon* **2011**, 49, 793-803.

[22] Pascual, J.; Peris, F.; Boronat, T.; Fenollar, O.; Balart, R. *Polym. Eng. Sci.* **2012**, 733-740.

[23] Yasin, T.; Nisar, M.; Shafiq, M.; Nho, Y.C.; Ahmad, R.C. *Polym. Compos.* **2013**, 34, 408-416.

[24] Zhang, W.D.; Shen, L.; Phang, I.Y.; Liu, T. *Macromolecules* **2004**, 37, 256-259.

[25] Zhang, C.; Tjiu, W.W.; Liu, T.; Lui, W.Y.; Phang, I.Y.; Zhang, W.D. *J. Psych. Chem. B* **2011**, 115, 3392-3399.

[26] Kunz, J.; Studer, M. *Kunstst. Int.* **2006**, 6, 92-94.

[27] Sponagel, S.; Unger, J.; Spies, K.H. *Kaut. Gummi Kunstst.* **2003**, 56, 608-613.

[28] Lin, J.; Wang, L.; Chen, G. *Tribol. Lett.* **2011**, 41, 209-215.

[29] Wagner, J.R.; Mount, E.M.; Giles, H.F. In The Definitive Processing Guide and Handbook. Extrusion – Polymer Selection for Coextrusion; Giles, H.F.; Wagner, J.R.; Mount E.M., Eds.; Elsevier, Oxford, **2014**, pp. 477-488.

[30] Qiu, L.; Yang, X.; Gou, X.; Yang, W.; Ma, Z.F.; Wallace, G.G.; Li, D. *Chem. Eur. J.* **2010**, 16, 10653-10658.

[31] Tian, L.; Meziani, M.J.; Lu, F.; Kong, C.Y.; Cao, L.; Thorne, T.J.; Sun, Y.P. *Appl. Mater. Interfaces* **2010**, 2, 3217-3222.

[32] Potts, J.; Dreyer, D.R.; Bielawski, C.W.; Ruoff, R.S. *Polymer* **2011**, 52, 5-25.

[33] Huang, H.; Liu, C.H.; Wu, Y.; Fan, S. *Adv. Mater.* **2005**, 17, 1652-1656.

[34] Shokrieh, M.M.; Hosseinkhani, M.R.; Naimi-Jamal, M.R.; Tourani, H. *Polym. Test.* **2013**, 32, 45-51.

[35] Musil, J. In Nanostructured Hard Coatings – Physical and mechanical properties of hard nanocomposite films prepared by reactive magnetron sputtering; Cavaleiro, A.; De Hosson, J.T.M. Eds.; Kluwer Academic/Plenum Publishers, New York, **2006**, pp. 407-463.

[36] J. Schiøtz, Simulations of nanocrystalline metals at the atomic scale. What can we do? What can we trust?, Proceedings of the 22nd Ris International Symposium on Materials Science (2001) 127-139.

[37] T.K. Gupta, B.P. Singh, R.B. Mathur, S.R. Dhakate, Multi-walled carbon nanotube-graphene-polyaniline multiphase nanocomposite with superior electromagnetic shielding effectiveness, Nanoscale 6 (2014) 842-851.

[38] Pan, M.; Shi, X.; Li, X.; Hu, H.; Zhang, L. *J. Appl. Polym. Sci.* **2004**, 94, 277-286.

[39] Wegrzyn, M.; Juan, S.; Benedito, A.; Gimenez, E. *J. Appl. Polym. Sci.* **2013**, 130, 2152-2158.
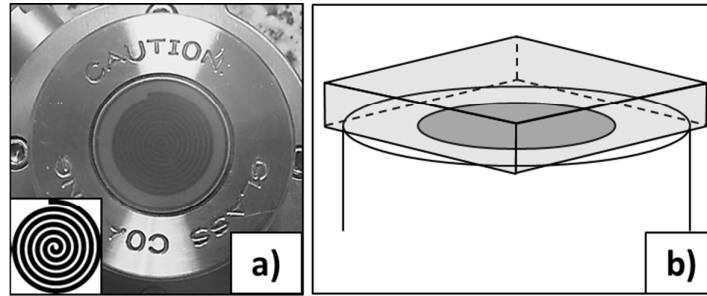
FIGURE 1: Methodology of thermal conductivity determination in hybrid PC-MWCNT/GnP nanocomposites: a) top-view on the sensor with a pictogram showing the sensor outlay, b) sample (gray) position on the sensor during measurement.
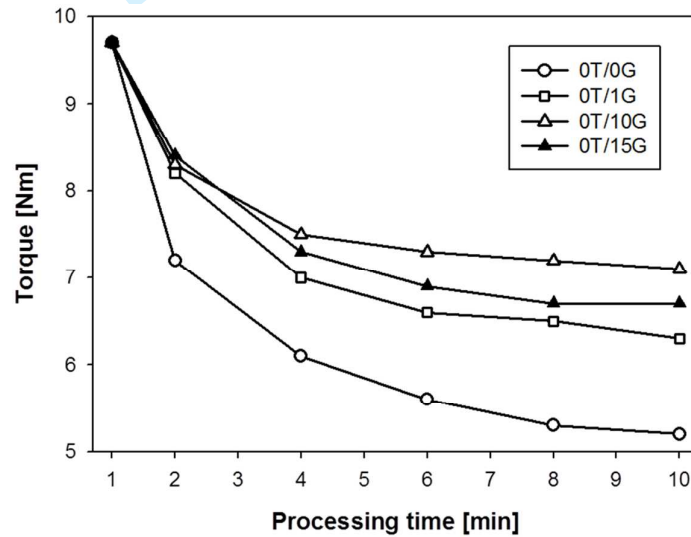

FIGURE 2: Torque during formation of PC-GnP nanocomposites at various processing stages.
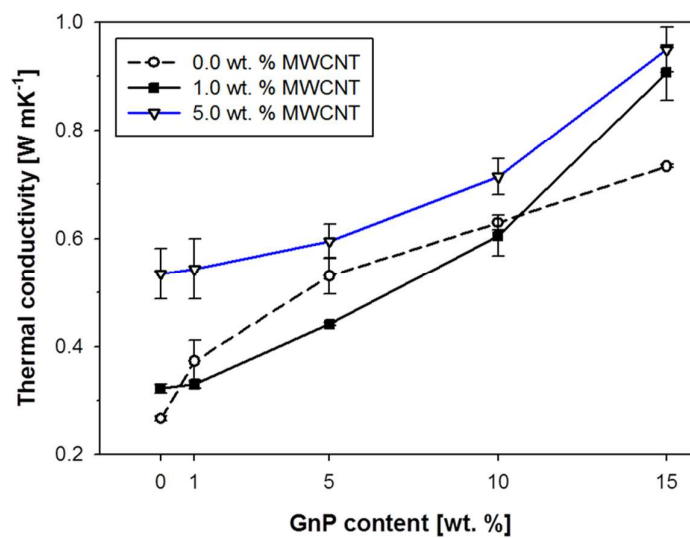
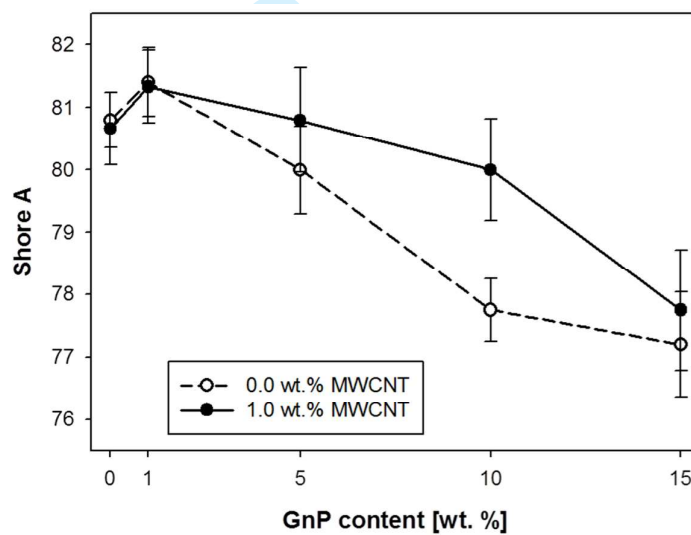**FIGURE 3:** Thermal conductivity of PC-MWCNT/GnP hybrid nanocomposites.

FIGURE 4: Shore A hardness of selected PC-MWCNT/GnP hybrid nanocomposites.
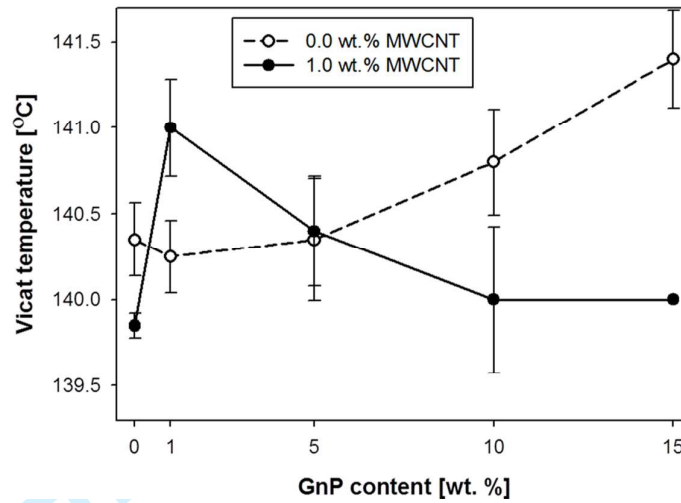
FIGURE 5: Vicat softening temperature of selected PC-MWCNT/GnP hybrid nanocomposites.
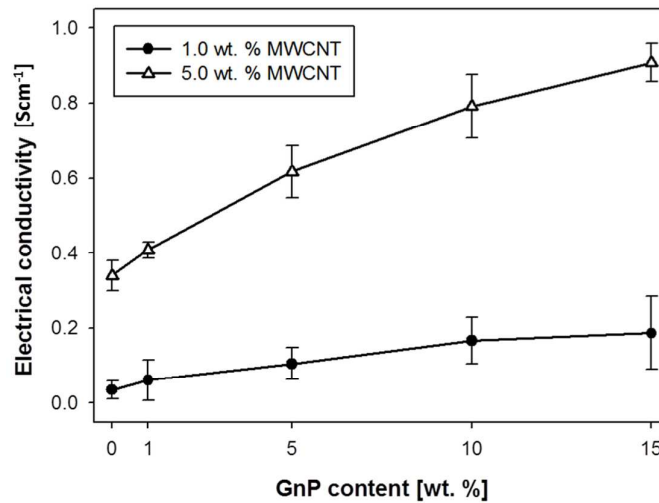

FIGURE 6: Electrical conductivity of selected PC-MWCNT/GnP hybrid nanocomposites.

Table 1: Samples codification and nanofillers content in prepared PC-MWCNT/GnP hybrid nanocomposites.

Sample code	Content	
	MWCNT	GnP
0T/0G	0.0 wt. %	0.0 wt. %
0T/1G	0.0 wt. %	1.0 wt. %
0T/5G	0.0 wt. %	5.0 wt. %
0T/10G	0.0 wt. %	10.0 wt. %
0T/15G	0.0 wt. %	15.0 wt. %
1T/0G	1.0 wt. %	0.0 wt. %
1T/1G	1.0 wt. %	1.0 wt. %
1T/5G	1.0 wt. %	5.0 wt. %
1T/10G	1.0 wt. %	10.0 wt. %
1T/15G	1.0 wt. %	15.0 wt. %
5T/0G	5.0 wt. %	0.0 wt. %
5T/1G	5.0 wt. %	1.0 wt. %
5T/5G	5.0 wt. %	5.0 wt. %
5T/10G	5.0 wt. %	10.0 wt. %
5T/15G	5.0 wt. %	15.0 wt. %

Table 2: Torque during formation of hybrid PC nanocomposites filled with various quantities of GnP and MWCNT.

Sample	Torque			
	4 min	6 min	8 min	10 min
1T/0G	6.5 Nm	6.3 Nm	6.0 Nm	6.0 Nm
1T/1G	7.5 Nm	7.3 Nm	7.0 Nm	6.8 Nm
1T/5G	8.6 Nm	7.8 Nm	7.5 Nm	7.4 Nm
1T/10G	9.8 Nm	8.8 Nm	7.8 Nm	7.5 Nm
1T/15G	9.5 Nm	8.5 Nm	7.7 Nm	7.4 Nm
5T/0G	9.9 Nm	8.4 Nm	8.2 Nm	7.8 Nm
5T/1G	10.9 Nm	9.5 Nm	8.6 Nm	7.9 Nm
5T/5G	11.1 Nm	9.7 Nm	8.7 Nm	8.0 Nm
5T/10G	11.2 Nm	9.9 Nm	8.7 Nm	8.2 Nm
5T/15G	11.4 Nm	10.1 Nm	9.1 Nm	8.6 Nm

Table 3: Thermal effusivity of PC-MWCNT/GnP nanocomposites measured at 26.1 °C (± 0.5).

Sample code	Effusivity [$Ws^{1/2}m^{-2}K^{-1}$]
0T/0G	610.57 (± 5.77)
0T/1G	729.26 (± 42.01)
0T/5G	860.00 (± 36.02)
0T/10G	990.22 (± 13.57)
0T/15G	1087.50 (± 2.93)
1T/0G	673.87 (± 9.73)
1T/1G	682.82 (± 8.93)
1T/5G	801.67 (± 33.17)
1T/10G	966.96 (± 37.64)
1T/15G	1252.13 (± 50.46)
5T/0G	906.79 (± 78.26)
5T/1G	935.56 (± 56.77)
5T/5G	957.57 (± 31.22)
5T/10G	1069.70 (± 31.46)
5T/15G	1275.19 (± 35.36)

Table 4: Modulus of elasticity in compression determined from Shore A hardness.

Sample code	Modulus of Elasticity [MPa]
0T/0G	12.89 (± 0.70)
0T/1G	13.23 (± 0.71)
0T/5G	12.46 (± 0.67)
0T/10G	11.40 (± 0.62)
0T/15G	11.17 (± 0.60)
1T/0G	12.81 (± 0.69)
1T/1G	13.19 (± 0.71)
1T/5G	12.89 (± 0.70)
1T/10G	12.46 (± 0.67)
1T/15G	11.40 (± 0.62)

Table 5: Electrical conductivity of selected PC-MWCNT/GnP nanocomposites.

Sample code	Electrical conductivity [Scm^{-1}]
0T/0G	1.00 E-14 (± 4.84 E-14)

0T/1G	1.04 E-10 (± 2.38 E-10)
0T/5G	7.59 E-08 (± 1.79 E-06)
0T/10G	2.53 E-05 (± 2.85 E-05)
0T/15G	5.60 E-04 (± 8.84 E-04)